

A NEW SCHEME FOR ELECTRO-OPTIC SAMPLING AT RECORD REPETITION RATES: PRINCIPLE AND APPLICATION TO THE FIRST (TURN-BY-TURN) RECORDINGS OF THz CSR BURSTS AT SOLEIL

E. Roussel*, C. Evain, M. Le Parquier, C. Szwaj, S. Bielawski
 PhLAM/CERLA, Villeneuve d'Ascq, France

L. Manceron, J.-B. Brubach, M.-A. Tordeux, J.-P. Ricaud, L. Cassinari,
 M. Labat, M.-E Couprie, P. Roy, Synchrotron SOLEIL, Gif-Sur-Yvette, France

Abstract

The microbunching instability is an ubiquitous problem in storage rings at high current density. However, the involved fast time-scales hampered the possibility to make direct real-time recordings of these structures. When the structures occur at a cm scale, recent works at UVSOR [1], revealed that direct recording of the coherent synchrotron radiation (CSR) electric field with ultra-high speed electronics (17 ps) provides extremely precious informations on the microbunching dynamics. However, when CSR occurs at THz frequencies (and is thus out of reach of electronics), the problem remained largely open. Here we present a new opto-electronic strategy that enabled to record series of successive electric field pulses shapes with picosecond resolution (including carrier and envelope), every 12 ns, over a total duration of several milliseconds. We also present the first experimental results obtained with this method at Synchrotron SOLEIL, above the microbunching instability threshold. The method can be applied to the detection of ps electric fields in other situations where high repetition rate is also an issue.

INTRODUCTION

The past decade has seen the rapid development of CSR studies in many storage rings. Despite the large amount of experimental observations, e.g. the recordings of coherent THz bursts, lack of direct observation of the electron bunch and its microstructures is a main issue to the test and the development of the theoretical models. Even though first real time measurements of CSR pulses using a YBCO superconductor-based detector at UVSOR-III have been successfully achieved [1, 2], a majority of storage rings emits coherent synchrotron radiation at higher frequencies than the state-of-the-art oscilloscope bandwidth (currently 65 GHz), e.g. ≈ 300 GHz at SOLEIL [3], ≈ 250 GHz at ANKA [4], ≈ 500 GHz at ELETTRA [5].

The electro-optic sampling (EOS) technique offers the possibility to measure THz electric fields with a sub-picosecond resolution. This technique has already been applied in storage rings [6–8]. However, to date, used methods based on electro-optic detection do not fulfill the requirements for a single-shot detection of CSR pulses at high-repetition rate, i.e. in the tens of megahertz (typical order of magnitude of electron bunch revolution frequency).

* eleonore.roussel@ed.univ-lille1.fr

At first, we recall the principle of the spectrally-encoded electro-optic (EO) technique for the single-shot detection of THz CSR pulses. Then, we show the potential interest of photonic time-stretch [9, 10], well-known in optics and photonics, for the EO techniques to overcome the limitation of acquisition rate needed in storage rings. Finally, we present experimental data obtained at SOLEIL using the time-stretch EO strategy.

SPECTRALLY ENCODED ELECTRO-OPTIC DETECTION

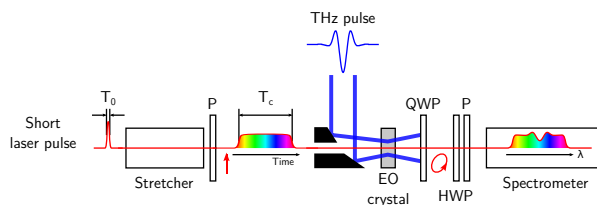


Figure 1: Schematic drawing of spectrally encoded electro-optic detection.

The spectrally-encoded electro-optic detection technique (EOSD) allows single-shot measurements of THz pulses (Fig. 1). In this technique, a probe laser pulse is stretched in a dispersive material or using a grating stretcher to a duration similar to the THz pulse duration before co-propagating in the EO crystal. In these conditions, the instantaneous frequency in the laser pulse varies with time. Thus, a modulation in time of the laser pulse induces the same modulation in the optical spectrum. The THz pulse induces a time dependent birefringence in the EO crystal through the Pockels effect and this anisotropy modulates the polarization state of the probe laser pulse which is converted into an amplitude modulation by a series of quarter-wave plate (QWP), half-wave plate (HWP) and a polarizer (P). The temporal modulation of the laser pulse is retrieved by measuring the spectrum of the laser pulse using a spectrometer and a photodiode array detector. The temporal resolution T_{min} of the EOSD is limited and is given by [11]

$$T_{min} = \sqrt{T_0 T_C}, \quad (1)$$

with T_0 the bandwidth-limited pulse duration (i.e. the pulse duration before the stretcher) and T_C the chirped probe laser pulse duration.

Even though the spectrally encoded EOSD allows single-shot measurements, the acquisition rate is limited by the speed of the current camera of at best around hundred kilohertz.

PHOTONIC TIME-STRETCH

Principle

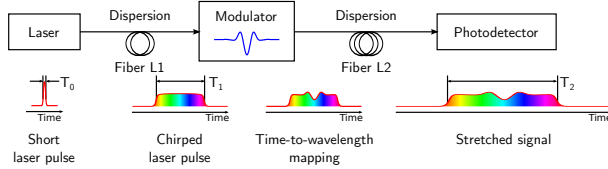


Figure 2: General principle of the photonic time-stretch process.

The principle of time-stretch process is simple and consists in slowing down a signal before the detection. A practical way to implement the time-stretch process is to use the photonic time-stretch technique shown in Fig. 2 [10]. The stretch process consists of two steps. The first step is the time-to-wavelength mapping where an intensity modulation is imprinted in a chirped laser pulse. This step can be compared to the spectrally encoded electro-optic scheme (Fig. 1). When a temporal modulation is imprinted in the chirped laser pulse, it is converted into the optical spectrum. The chirped pulse is obtained by propagating a short laser pulse in a dispersive medium, here an optical fiber of length L_1 . The chirped pulse duration is given by $T_1 = \Delta\lambda D_1 L_1$ with $\Delta\lambda$ the optical bandwidth of the laser pulse and D_1 the dispersion parameter of the fiber which is in units of $\text{ps}\cdot\text{nm}^{-1}\cdot\text{km}^{-1}$. The second step is the wavelength-to-time mapping performed by the second fiber. The modulated chirped pulse propagates through a second dispersive medium, here a fiber of length L_2 . The temporal modulation in the pulse is stretched as the chirped laser pulse is further chirped along the fiber. Finally, the temporal waveform is stretched in time so that it is slow enough to be detected using a photodiode. The pulse duration T_2 is expressed as follows [9]:

$$T_2 = T_1 + \Delta\lambda D_1 L_2 = \left(1 + \frac{L_2}{L_1}\right) T_1 = M \times T_1 \quad (2)$$

where M is called the stretch factor or magnification factor.

Trade-off Between Stretch Factor and Acquisition Rate

The time-stretch process allows to measure the optical spectrum using a photodiode instead of a spectrometer and a photodiode array detector (Fig. 3). As can be seen in Fig. 3(a,b), the temporal shape of the stretched pulse after the second fiber of length $L_2 = 2$ km is almost identical to the optical spectrum. The stretched pulse duration, equal to ≈ 4 ns, is clearly temporally resolved with the balanced detector of 20 GHz bandwidth. Furthermore, single-shot with

high-acquisition rate is possible contrary to the measurements using a spectrometer with camera. In Fig. 3(c), the repetition rate of the laser pulse is 88 MHz and thus, single-shot acquisition is performed every 11 ns. Additionally, the use of photodiode enables to implement the balanced detection scheme which is not possible with a spectrometer with camera [12].

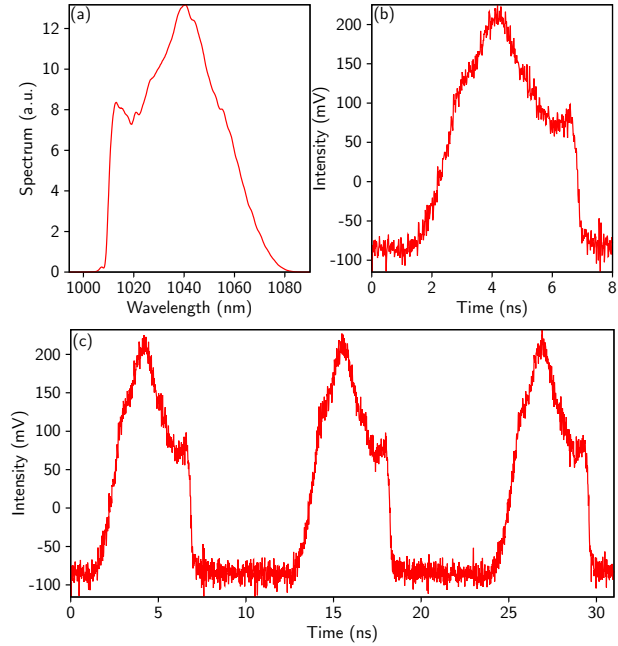


Figure 3: (a) Average spectrum of an Yb fiber laser and (b) associated temporal signal of the stretched laser pulse (after propagation in a 2 km fiber). Note that the long wavelengths arrive first, the temporal shape is identical but reversed compared to the spectral shape. (c) Successive stretched laser pulses at a repetition rate of 88 MHz.

Bandwidth Limitations

As for the usual spectral-encoding measurements with spectrometers, the time-stretch has a limited temporal resolution. The bandwidth of the system is limited by the dispersion penalty [9] which is described by the transfer function [9, 13]:

$$H(f_m) = \cos^2\left(2\pi^2\beta_2\frac{L_2}{M}f_m^2\right) \approx \cos^2\left(2\pi^2\beta_2L_1f_m^2\right), \quad (3)$$

for stretch factors $M \gg 1$. β_2 is the group velocity dispersion of the fiber and is linked to the dispersion parameter $D_1 = -2\pi c\beta_2/\lambda^2$. f_m is the main frequency of the modulation signal, i.e. the main frequency of the THz field. The penalty dispersion may be viewed as an interference between the upper and lower sideband of the optical carrier created by the THz field modulation. The transfer function is represented in Fig. 4 for various fiber lengths. From the first zero of the transfer function, we can deduce the bandwidth of the

system at 3 dB

$$f_{max} = \sqrt{\frac{1}{8\pi\beta_2 L_1}}. \quad (4)$$

Note that this bandwidth is identical to the bandwidth of the traditional EOSD.

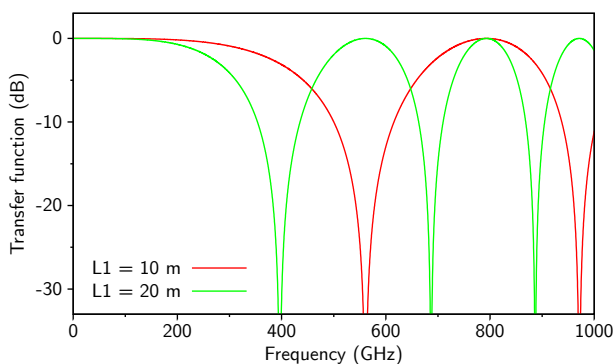


Figure 4: Transfer function induced by fiber dispersion using time-stretch for a fiber length (a) $L_1 = 10$ m and (b) $L_1 = 20$ m. The parameter β_2 is equal to $25.3 \cdot 10^{-27} \text{ s}^2/\text{m}$.

In summary, the time-stretch process highlights a trade-off between bandwidth and time aperture. Indeed, as we increase the time aperture T_1 by propagating in a longer fiber L_1 , the maximum frequency f_{max} that can be detected without distortion decreases.

EXPERIMENTAL RESULTS AT SYNCHROTRON SOLEIL

We have used this new electro-optic detection scheme to get single-shot measurements of THz CSR pulses with a high repetition rate. As described in the previous section, the technique is based on the traditional spectrally-encoded electro-optic detection (EOSD) associated to the photonic time-stretch process. This new technique, which we call time-stretched spectrally-encoded electro-optic detection (TS-EOSD), enables real-time recording, turn-by-turn of the THz CSR bursts. This TS-EOSD experiment has been set up at the AILES infrared beamline on Synchrotron SOLEIL. The storage ring was operating in single bunch mode and in nominal-alpha mode leading to a bunch length of 4.59 mm RMS. The beam current was set at $I = 15$ mA which is far above the microbunching instability threshold (around 10 mA).

Measurements with various fiber lengths have been performed which allow to vary the acquisition time window and the temporal resolution. The analysis of the temporal evolution of the CSR spectrum (Fig. 5) reveals that the main wavenumber of the instability is centered around 10 cm^{-1} . At higher frequency components, the CSR spectra are unfortunately altered by the transfer function of the system.

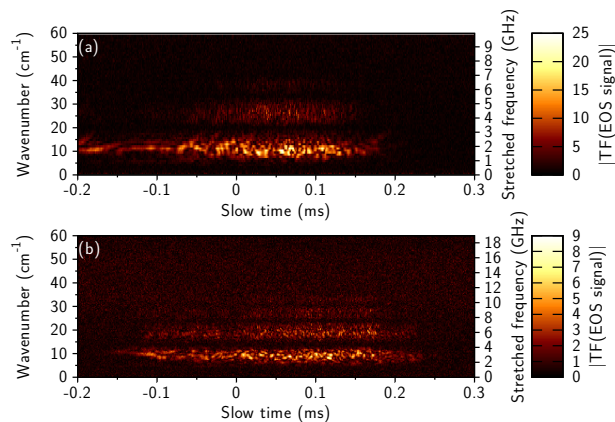


Figure 5: Temporal CSR spectra obtained with the time-stretch spectrally-encoded electro-optic detection technique for two fiber lengths: (a) $L = 10$ m and (b) $L = 20$ m. Note that the stretched frequency corresponds to detected frequencies on the oscilloscope. The real frequency (given in wavenumber) which corresponds to frequency range in the EO crystal is deduced using the magnification factor $M = 1 + L_2/L_1$.

CONCLUSION

The photonic time-stretch process is an elegant method to perform fast real-time spectroscopic measurements as the state-of-the-art photodetectors are much faster than traditional spectrometers. Thus, we have reported the real-time, turn-by-turn, monitoring of CSR pulses emitted during the microbunching instability at Synchrotron SOLEIL using a new opto-electronic strategy based on the spectrally-encoded electro-optic detection scheme associated to the photonic time-stretch.

ACKNOWLEDGMENT

The work was supported by the ANR (Blanc 2010-042301). The CERLA is supported by the French Ministère chargé de la Recherche, the Région Nord-Pas de Calais and the FEDER.

REFERENCES

- [1] E. Roussel *et al.*, "First Direct, Real Time, Recording of the CSR Pulses Emitted During the Microbunching Instability, using Thin Film YBCO Detectors at UVSOR-III", IPAC'14, Dresden, Germany, MOPRO056, This Conference.
- [2] J. Raasch *et al.*, "Electrical Field Sensitive High- T_C YBCO Detector for Real-Time Observation of CSR", IPAC'14, Dresden, Germany, THPME125, This Conference.
- [3] C. Evain *et al.*, Europhys. Lett. **98**, 40006 (2012).
- [4] V. Judin *et al.*, "Spectral and temporal observations of CSR at ANKA", IPAC'12, New Orleans, USA, TUPPP010 (2012).
- [5] E. Karantzoulis *et al.*, Infrared Physics and Technology **53**, 300 (2010).
- [6] I. Katayama *et al.*, Applied Physics Letters **100**, 111112 (2012).

- [7] F. Müller *et al.*, Phys. Rev. ST Accel. Beams **15**, 070701 (2012).
- [8] N. Hiller *et al.*, “Electro-optical Bunch Length Measurements at the ANKA Storage Ring”, IPAC’13, Shanghai, China, MOPME014 (2013).
- [9] F. Coppinger *et al.*, IEEE Transactions on Microwave Theory and Techniques **47**, 1309 (1999).
- [10] Y. Han and B. Jalali, Journal of Lightwave Technology **21**, 3085 (2003).
- [11] F.G. Sun, Z. Jiang and X.-C. Zhang, Applied Physics Letters **73**, 2233–2235 (1998).
- [12] J.H. Wong *et al.*, Journal of Lightwave Technology **29**, 3099–3106 (2011).
- [13] Y. Han and B. Jalali, IEEE Transactions on Microwave Theory and Techniques **51**, 1886–1892 (2003).